Since January 2020 Elsevier has created a COVID-19 resource centre with free information in English and Mandarin on the novel coronavirus COVID-19. The COVID-19 resource centre is hosted on Elsevier Connect, the company's public news and information website.

Smart Health 26 (2022) 100308

Contents lists available at ScienceDirect

Smart Health

journal homepage: www.elsevier.com/locate/smhl

An intelligent spatial stream processing framework for digital forensics amid the COVID-19 outbreak

Sujit Bebortta [a], Aditya Ranjan Dalabehera [a], Bibudhendu Pati [b], Chhabi Rani Panigrahi [b], Gyana Ranjan Nanda [a], Biswajit Sahu [a], Dilip Senapati [a,*]

[a] Department of Computer Science, Ravenshaw University, Cuttack, 753003, Odisha, India
[b] Department of Computer Science, Rama Devi Women's University, Bhubaneswar, 751022, Odisha, India

ARTICLE INFO

Keywords:
COVID-19
Event triggered video framing (ETVF)
Real-time video framing (RTVF)
Autocorrelation
Queuing theory
Poisson process

ABSTRACT

In recent times, several strategies to minimize the spread of 2019 novel coronavirus disease (COVID-19) have been adopted. Some recent technological breakthroughs like the drone-based tracking systems have focused on devising specific dynamical approaches for administering public mobility and providing early detection of symptomatic patients. In this paper, a smart real-time image processing framework converged with a non-contact thermal temperature screening module was implemented. The proposed framework comprised of three modules *viz*., smart temperature screening system, tracking infection footprint, and monitoring social distancing policies. This was accomplished by employing Histogram of Oriented Gradients (HOG) transformation to identify infection hotspots. Further, Haar Cascade and local binary pattern histogram (LBPH) algorithms were used for real-time facial recognition and enforcing social distancing policies. In order to manage the redundant video frames generated at the local computing device, two holistic models, namely, event-triggered video framing (ETVF) and real-time video framing (RTVF) have been deduced, and their respective processing costs were studied for different arrival rates of the video frame. It was observed that the proposed ETVF approach outperforms the performance of RTVF by providing optimal processing costs resulting from the elimination of redundant data frames. Results corresponding to autocorrelation analysis have been presented for the case study of India pertaining to the number of confirmed COVID-19 cases, recovered cases, and deaths to obtain an understanding of epidemiological spread of the virus. Further, choropleth analysis was performed for indicating the magnitude of COVID-19 spread corresponding to different regions in India.

1. Introduction

The rapid spread of the 2019 novel coronavirus disease (COVID-19) was observed to be one of the deadliest pandemic outbreaks of human history in terms of the number of nations affected. It started in December 2019 with a possible contamination of bat meat carrying the viral pathogen and later came in contact of the human population (Sarkodie & Owusu, 2020; Singhal, 2020). Since then the disease has spread to almost every country in the world making it the most dreaded health issue (Das & Bebortta, 2022; Li et al., 2020; Team, 2020). The number of cases spike with time every week during the peak period of the pandemic had imposed challenges on the medical facilities, number of healthcare personnel involved and the shortage of equipment made it even harder for the situation to be dealt with (Guan et al., 2020; Huang et al., 2020; Lau & Xiong, 2020; Organization et al.,

* Corresponding author.
E-mail address: dilipsenapati.cs@ravenshawuniversity.ac.in (D. Senapati).

https://doi.org/10.1016/j.smhl.2022.100308
Received 27 March 2022; Received in revised form 17 July 2022; Accepted 8 August 2022
Available online 12 August 2022

2020; Peng, Ho, & Hota, 2020; Sahu, Mishra, & Lal, 2020). Since the outbreak of COVID-19 the role of drone based medication and food supply, monitoring, surveillance of crowded areas and much more have gained much popularity. Some recent studies have exploited digital forensic analysis towards processing of voluminous digital imagery for facilitating facial identification and inferring some data in acquaintance of interest (Domingues & Rosário, 2019; Garfinkel, 2010). In perspective of COVID-19, digital forensic has played a pivotal role in identifying facial mask and for facial recognition of COVID-19 suspects (Quick & Choo, 2014). However, in order to capture the massive digital data being generated from systems deployed for COVID-19 tracking, the present digital forensic analysis techniques face challenges in handling its growing demands of data acquisition and for processing over low-powered devices (Bebortta, Singh, & Senapati, 2022). Thus, in this perspective, the present work proposes a mathematical framework towards managing the computational overheads in digital forensic analysis and minimizing service costs for processing the data packets generated from facial recognition module.

In this paper, we propose three modules for management of digital forensic data towards assisting facial recognition in COVID-19 tracking systems. First is a smart thermometer gun that would have a camera synced to the gun or working in accordance with the gun that captures the photo only when the gun triggers it. Secondly, a smart quarantine monitoring and identifying infection hotspot which would deploy a drone-based facial recognition platform Local Binary Patterns Histogram LBPH (Ahonen, Hadid, & Pietikainen, 2006) for identifying (Hsu & Chen, 2015) and Haar Cascade human face detection (Singh, Shokeen, & Singh, 2013) for tracking the movements of the person infected with the virus (Iqbal, Alam, Kazim, MacDermott, et al., 2019; Nguyen et al., 2019; Sahoo, Senapati, Thakur, & Naik, 2020; Unlu, Zenou, Riviere, & Dupouy, 2019) and advised to stay in self-isolation, if the person is found breaking the regulations, an alert will be generated. The person will be tracked, making it easier to follow if the carrier person has infected any other individual. Thirdly, social distancing powered by drones which will have a Histogram of Oriented Gradients (HOG) human detection mechanism (Nguyen, Li, & Ogunbona, 2016) attached and the drones are to hover at the areas with a high possibility of gathering, the drone would broadcast a warning, or the police are to alerted if the social distancing is not followed. The simulated experiments are carried out using OpenCV (Fan, Zhang, Wang, & Lu, 2012), and the Raspberry pi (Mathur, Subramanian, Jain, Choudhary, & Prabha, 2017) over a mobile workstation. These modules will be effective in containing the spread of the virus and bringing the computing costs for the operations down significantly (Bebortta, Panda and Panda, 2020; Buizza, 2020; Ditlevsen & Samson, 2013; Goel & Richter-Dyn, 2016). Considering the number of infected persons in the area and studying the local recovery rate, we propose an event-triggered video framing mechanism (ETVF) and the conventional real-time video framing framework (RTVF) is taken into consideration for defining the merits of our proposed framework. After that, an extensive comparative study based on simulations is demonstrated regarding the service cost of both the paradigms (Bebortta & Senapati, 2021a; Bebortta, Senapati, Panigrahi, & Pati, 2021a, 2021b; Bebortta & Singh, 2021). An event-based frame transmission (EBFT) algorithm is proposed, which results in computing the service cost by considering the average arrival rate and service rate of the video frames. Further, the numerical results corresponding to the proposed ETVF and the RTVF model have been provided. It is observed that the ETVF model greatly outperforms the RTVF model by providing minimal service costs for processing the video frames. Autocorrelation analysis has been performed for the case study of India pertaining to the number of confirmed COVID-19 cases, recovered cases, and deaths reported over a specific interval of time. Further, choropleth analysis has been performed for indicating the magnitude of the COVID-19 spread corresponding to different regions in India (Das & Bebortta, 2022). It gives a clear picture of how the proposed model could be helpful in the present scenario in terms of cost-effectiveness and the speed at which the security response can be made available, protecting the life of masses from the outbreak. The drone network significantly saves the costs for patrolling by minimizing the police van movements, and the drones can be operated remotely and effectively (Bebortta & Das, 2020; Bebortta et al., 2021b, 2020; Boland et al., 2020; Mukherjee & Senapati, 2022; Mukherjee, Singh, & Senapati, 2019) with the energy harvesting facilities that would give them a longer battery life and more service time (Mirzaeinia, Hassanalian, Lee, & Mirzaeinia, 2019).

1.1. Contributions

The major contributions of this study can be summarized as follows:

- A COVID-19 tracking system based on digital forensics a three-tiered framework was proposed for detection of temperature, facial recognition, and social distance monitoring.
- A smart tracking system that captures data by exploiting the Raspberry pi 5MP camera module and MLX-90614 based contactless infrared (IR) thermometer was provided.
- The LBPH and HOG algorithms were implemented in the OpenCV platform to facilitate facial recognition and monitoring of social distancing in the proposed experimental set up.
- A comparative study of the proposed ETVF and RTVF models was provided to obtain a better understanding on the analytical aspects of managing the redundant video frames captured from the proposed experimental scenario.
- Autocorrelation analysis and mapping of COVID-19 hotspots over the geographic limits of India was studied to obtain an overview and for better understanding of the epidemiological spread of the virus and its growth over time.
- Numerical illustrations to study cost analysis of the proposed ETVF and RTVF models for processing the optimal video frames with a specific arrival rate was presented.
- Finally, a comparative study for the computational complexity of some state-of-the-art algorithms used for human movement tracking was obtained in convergence with the proposed algorithm, where the proposed approach obtained a computational complexity of the order, $O(n)$.

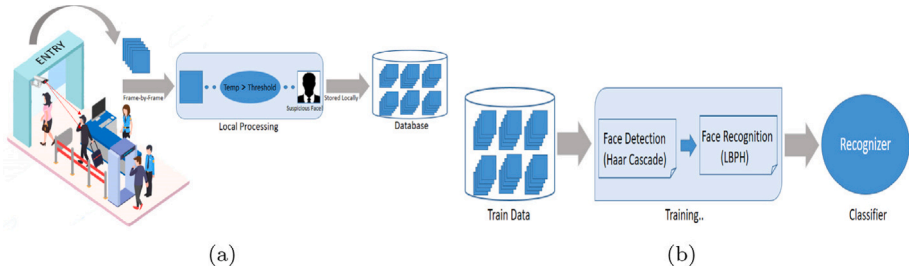

Fig. 1. (a) Smart screening facility. (b) Training the dataset to generate the recognizer.

The paper comprises of 6 sections starting with a brief introduction related to digital forensics and drone computing in Section 1 followed by the proposed modules in Section 2. After that, in Section 3, we formulate a problem domain based on the current scenario and provide its solutions. The autocorrelation function of three empirical datasets corresponding to the number of confirmed cases, number of new recovered cases, and number of new death cases has been formulated in Section 4. Section 5 is the results and discussions which provide real-time results for implemented framework and also evidence comparisons between the existing conventional framework and the proposed ETVF model. Lastly, in Section 7, the conclusive remarks and the future research directions have been provided.

2. Proposed frameworks

In this section, we introduce the proposed modules and the deployment architecture of the same in the urban and rural environments to help the administration in monitoring and maintaining the necessary precautionary guidelines issued by government agencies, namely self-isolation or home quarantine, social distancing, etc. We also elaborate on the compliance of the proposed models with the existing situation that has been prevailing all around the world and a comparative study considering the beneficial aspects of the modules are discussed concerning economic and operating advantages.

2.1. Motivations

The extensively growing popularity of the applications of drone technology in some of the most crucial areas like transportation management, public safety, national security, etc. have encouraged the institutions to use the drone in every other aspect of life (Bebortta & Senapati, 2021b). Likewise, real-time image processing is also a significant asset when it comes to the field of surveillance, even under hostile conditions in a time like this when the unmanned ventures come in handy and save lives in desperate situations where a single human contact might bring the fate of an entire city under darkness. A drone equipped with the image processing platform and with reliable service and significantly low operating costs is the need of the hour. Such a measure could reduce human interaction and provide trustworthy assistance for monitoring and management in such a desperate time where the lives of people are on the line.

2.2. Smart temperature screening system

This module has two components, one is the thermometer gun, and the other is the camera. The thermometer gun is used in measuring the body temperature of the person who is either moving from places where the outbreak has been severe. Many such individuals might exhibit a suspicious body temperature or, in some cases, very mild symptoms. Regardless of that, each person has to pass through the temperature screening process with an official pointing the temperature gun at the individuals or of the fixed thermal camera is in place to continuously relay the body temperature of persons passing through the facility. The proposed model moves one step ahead by incorporating a local processing for event-triggered camera (Hu, Delbruck, & Liu, 2020; Monforte, Arriandiaga, Glover, & Bartolozzi, 2020), which is scheduled to operate whenever the output from the thermometer gun reaches a specified threshold value owing to which the camera captures only the photos of the individuals showing some abnormality in body temperature leading to the danger of a possible infection. In other words, the camera is triggered to capture the image only when the threshold temperature is crossed. The image captured is stored in a database of people who might have been exposed to the virus. The images stored in the database are used as the training datasets for the recognizer that is to be used in the next modules for tracking the infection footprint (Bebortta & Singh, 2022a, 2022b). This makes it easier for the administration and the medical staff to identify the person right after they enter the city, which facilitates a thorough examination of their whereabouts and better medical assistance is imparted.

The Fig. 1-a demonstrates the setup of the screening facility where the persons pass through the screening, and the local processing mechanism continuously checks if the output temperature reading crosses the threshold, the camera is triggered to capture the image of the respective person and then stores the image in the database. Fig. 1-b shows the mechanism of storing images in the database for training the model using Haar Cascade algorithm and LBPH algorithm for facial recognition to generate the recognizer,

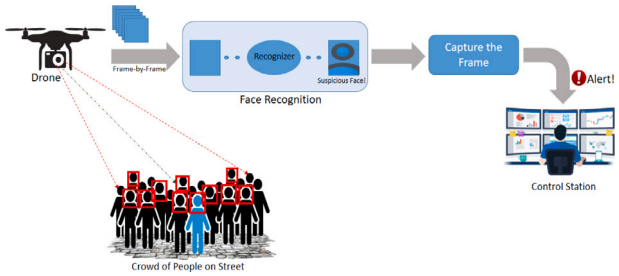

Fig. 2. Tracking the infected individual and alert generation.

which is later used in the next stage of the proposed module. The significant advantage of such a system is to minimize the number of human resources involved as the entire system functions autonomously, relying on the local drone computing and the event triggered video framing architecture; thereby, the exposure of the officials at work is highly reduced. This system also speeds up the entire procedure of identifying suspected individuals who need potential medical attention.

2.3. Tracking infection footprint

This module provides the working principle of facial recognition and detection. This paradigm is crucial in monitoring the individual who are suspected of carrying the pathogen. The persons who have passed through the screening facility and have exhibited suspicious temperature or mild symptoms are advised to practice self-isolation and to stay indoors during a latent period or incubation period for not affecting others in the locality, thereby preventing the community transmission of the disease. Still, a few irresponsible individuals do not obey the regulations and dare to come out, thereby threatening the safety of others even with the strict patrolling of the local police. But the police and other ground surveillance team are humans too, and they have chances of getting infected with too much exposure, and even with strict precautions and the continuous patrolling can be very costly. To encounter such a nuisance, drone surveillance is the best remedy to check and track the movements of the quarantines at all times. The proposed framework is drone surveillance network (Motlagh, Bagaa, & Taleb, 2017) equipped with a human detection (Bold, Sosorbaram, & Lee, 2016) and facial recognition mechanism using the HOG human body detection (Saika, Takahashi, Takeuchi, & Katto, 2016; Seemanthini & Manjunath, 2018) and Haar Cascade face detection algorithm (Cuimei, Zhiliang, Nan, & Jianhua, 2017) and real time LBPH facial recognition algorithm (Visakha & Prakash, 2018; Zhao & Wei, 2017), the recognizer is trained with images from the datasets created with the images of the persons with the symptoms right from the smart screening facility and the datasets of the local hospitals. The drones are deployed at major hotspot areas where the number of the home quarantined is the most or at the places where the possibility of a gathering is maximum, for instance, at a medicine store or local vegetable market. The drone continuously monitors the area, and if the recognizer recognizes an individual, an alert is sent to the nearest security station and or even an audio warning is broadcasted. This is to all majority can be helpful in monitoring the movements of the infected person who has broken the self-isolation, and as soon as the recognizer finds a match, it also detects other humans in close proximity of the infected individual and sends the image of those persons to the database. This facility helps identify the footprint of the infection and proper examination of the persons who might have the possibility of getting infected while the victim broke the self-isolation. Thereby enhancing the response of the administration to the pandemic and providing well-organized security to the public. Fig. 2 shows the scenario of how the alert is generated after an infected individual is detected breaking the self-isolation and then capturing the images of others in close proximity of the infected person to queue them for medical examination and aid to curb the rapidly rising rate of the pandemic.

2.4. Monitoring social distancing

The entire planet is under the clutch of the COVID-19 as the major nations falter the frequency curve in providing both the medical and economic aid to their people (Wang, Horby, Hayden, & Gao, 2020). It is high time, we get the right thing done and take the much-needed provisions to save the mankind from the threat of this disease, and in a country like India where the dreaded pandemic is yet to enter the community transmission phase, precautionary measures are to be strictly followed to tackle the situation. With a population of 1.3 billion, it is a huge task to make the people follow the social distancing amidst the enormous population density. In a critical situation like this, proper monitoring is essential to impose the regulations and survey whether they are followed. The principle for social distancing has been prescribed as a minimum of 2 m distance from person to person at public places irrespective of the job the person is out for. Our proposed module specializes in monitoring whether the social distancing is followed at public places like markets, near a medicine store, and even the rural areas can be monitored, where there are negligence and ignorance towards the rules. The module is deployed with the drones equipped with the human detection mechanism, HoG descriptor for the human body detection (Davis & Sahin, 2016). The working principle of the paradigm is as follows, the drone surveys the location detecting human using the detection mechanism, and after that locally processes the video frames to calculate the distance between the detected individuals; let say the minimum distance has to be two meters, and if any

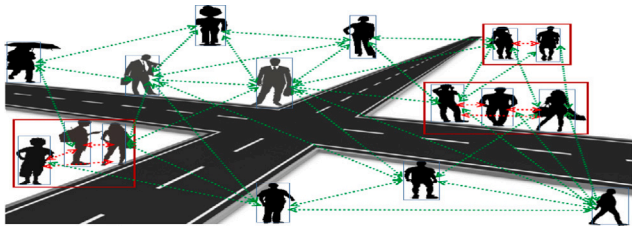

Fig. 3. Detection of Social distancing.

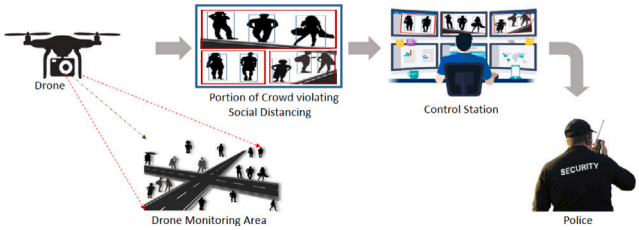

Fig. 4. Monitoring the Social distancing.

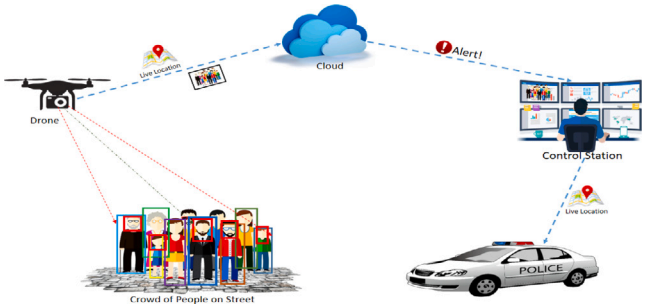

Fig. 5. Digital Forensics via drone.

deviation is encountered in the crowd the drone immediately relays the audio message that is fed into it. If the situation does not come to normal, an alert is forwarded to the nearest police station or the patrolling officers nearby. The local processing of the distance between the humans detected in a crowd makes the monitoring process faster and keeps the people in a safe distance at all time, and the monitoring through the drones makes it reach even the remote places and speeds the response time, and that is what matters when it comes to stopping the disease from spreading. The Fig. 3 demonstrates a scenario in a locality where the drone captured frame is processed locally to detect the distance between the people and determine the group not following the social distancing. The Fig. 4 demonstrates the order of the events happening right from monitoring people to deploying human detection and then determining the social distancing and then if not followed the alert is relays all the way to the surveillance center and then to the officials. The Fig. 5 shows the overall architecture of the digital forensic application, event triggered video framing (ETVF) and the human detection and facial recognition in monitoring the crowd and action by the control station in response to the alert generated by the drone. This infrastructure can even be helpful to trace the individuals who escape the government quarantine centers or flee the screening facility after being suspected to carry the virus. This system can effectively track them at their possible hideouts as soon as possible and prevent a certain outbreak in the area.

3. Problem formulation

The average pandemic rate (or the outbreak of a disease that spans a wide geographical location) is defined as $\lambda = \langle \lambda_i \rangle$, where λ_i pandemic rates of different locations. The average pandemic rate λ varies with time (i.e., time-dependent) because, during the latent period or incubation period, the number of susceptible persons may be infected persons (Bebortta, Singh, Mohanty and Senapati, 2020). Hence, λ is the average of infected persons identified in the video streaming, which follows the Poisson process and it is defined as Bebortta, Rajput and Pati (2020), Goel and Richter-Dyn (2016), Mukherjee, Nayak, and Senapati (2021), Mukherjee, Pati, and Senapati (2020), Nayak, Singh, and Senapati (2020), Senapati et al. (2016) and Singh, Senapati, Mukherjee and Rajput (2019)

$$P_x(t) = \frac{e^{-\lambda t}(\lambda t)^x}{x!}, \; x = 0, 1, 2, \ldots \tag{1}$$

where x is number of infected individuals in the population. As the infectious period can be reduced by the recovery of the infected individual, which reduces the number of event-triggered data frames with the passage of time. Similarly, the average service rate of event-triggered data frames follow the exponential distribution, and it is defined as

$$f(t) = \mu e^{-\mu t},\ t \geq 0. \tag{2}$$

where μ denotes the service rate for processing the event-triggered data frames.

3.1. Event triggered video framing (ETVF) model

The cost of processing of event-triggered video frames from the real-time video streaming is given by (Bebortta, Singh, Pati and Senapati, 2021)

$$C_{ET}(\mu) = \frac{c_1 \mu}{k} + c_2 N_1, \tag{3}$$

where k is the reduction factor of frames for real-time video steaming depending upon the risk of a person being infected by COVID-19, c_1 is the processing cost per data frames, c_2 is the waiting cost for each event-triggered frame before being uploaded to the cloud storage, and N_1 denotes the number of event-triggered frames generated by the local processor such that Trivedi (2008), $N_1 = \left(\frac{\lambda}{\mu-\lambda}\right)$. The reduction factor k takes a suitable value in minimizing the number of video frames transmitted to the cloud server. Hence, the reduction factor is inversely proportional to the isolation rate and the social distancing rate. The relationship of k corresponding to the self-isolation rate(α) and the social distancing rate(β) can be obtained as follows,

$$k \propto \frac{1}{(\delta)(\alpha) + (1-\delta)(\beta)} = \frac{\zeta}{(\delta)(\alpha) + (1-\delta)(\beta)},\ 0 \leq \delta \leq 1, \tag{4}$$

where ζ is the constant of proportionality. Using well-known queueing theory model $(M/M/1) : (\infty/FCFS)$ (Singh, Senapati, Bebortta and Rajput, 2019), the service cost model for event-triggered frames from the real-time video streaming is defined as,

$$C_{ET}(\mu) = c_1 \mu + c_2 \left(\frac{\lambda}{\mu - \lambda}\right). \tag{5}$$

Thus, the necessary condition for Eq. (5) is given by,

$$\frac{dC_{ET}}{d\mu} = c_1 - \frac{\lambda c_2}{(\mu-\lambda)^2} = 0, \tag{6}$$

The critical point Eq. (6) is obtained as,

$$\hat{\mu} = \lambda + \sqrt{\frac{\lambda c_2}{c_1}}. \tag{7}$$

Since, $\left.\frac{d^2 C_{ET}}{d\mu^2}\right|_{\mu=\hat{\mu}} = \frac{2\lambda c_2}{(\hat{\mu}-\lambda)^2} > 0$. Thus, the Eq. (7) attains optimal service rate at $\hat{\mu}$ for processing of the triggered frames.

3.2. Real-time video framing (RTVF) model

Similarly, the service cost for transmitting each data frames of real-time video streaming is stated as (Bebortta, Singh et al., 2021)

$$C_{RT}(\mu) = c_1 \mu + c_2 N_2, \tag{8}$$

where N_2 denotes the number frames capture from real-time video surveillance, and using the $\left(M/E_k/1\right) : (\infty/FCFS)$ model we have (Trivedi, 2008),

$$N_2 = \frac{k+1}{2k} \frac{\lambda^2}{\mu(\mu-\lambda)} + \frac{\lambda}{\mu}. \tag{9}$$

From Eqs. (8) and (9), we get

$$C_{RT}(\mu) = c_1 \mu + c_2 \left[\frac{k+1}{2k} \frac{\lambda^2}{\mu(\mu-\lambda)} + \frac{\lambda}{\mu}\right]. \tag{10}$$

Now from Eq. (10), we get,

$$\frac{dC_{RT}}{d\mu} = c_1 + c_2 \left(-\frac{\lambda}{\mu^2} - \frac{(k+1)(2\mu-\lambda)\lambda^2}{2k(\mu(\mu-\lambda))^2}\right), \tag{11}$$

Thus, the necessary condition for Eq. (11) for critical point is given by

$$\frac{dC_{RT}}{d\mu} = 0,\ \mu = \hat{\mu} \tag{12}$$

Differentiating Eq. (11) with respect to service rate, we get

$$\frac{d^2C_{RT}}{d\mu^2} = c_2\left(\frac{2\lambda}{\mu^3} - \frac{(k+1)\lambda^2(3\mu^2+\lambda^2-3\mu\lambda)}{k\mu^3(\mu-\lambda)^3}\right) \tag{13}$$

As $\left.\frac{d^2C}{d\mu^2}\right|_{\mu=\hat{\mu}} > 0$, the Eq. (8) attains its minimal value at $\mu = \hat{\mu}$.

3.3. Proposed frame transmission algorithm

The fundamental premise for evaluating the outbreak of the pandemic for any given location is determined by the average pandemic rate specific to any region i.e., λ, where $\lambda = \langle\lambda_i\rangle$ for ith locations. Hence, the number of patients infected with the COVID-19 virus is x, and the average pandemic rate, the probability of the average number of patients, can be identified over a specific temporal domain t through the proposed drone-based video streaming scheme obtained in Eq. (1). Algorithm 1 provides a generalized event-based frame transmission (EBFT) algorithm for the optimal number of video frames captured using the proposed scheme. Further, pertaining to the average rate of the infected persons identified through video streaming, the processing rate for each of the captured data frames can be determined as discussed in Eq. (2).

Algorithm 1: Optimal event based frame transmission (EBFT) algorithm.

Input : t, x, c_1, c_2, k;
Output : $C_{ET}(\mu), C_{RT}(\mu)$;

$x \leftarrow$ Number of infected persons in the population.
$\lambda \leftarrow$ Average pandemic rate per region.
$t \leftarrow$ Frame transmission time.
$P_x(t) \leftarrow$ Probability of identifying a person in video streaming.
$\mu \leftarrow$ Average service rate for processing the data frames.
$f(t) \leftarrow$ Probability density function for the average service rate.
$k \leftarrow$ Reduction factor.
$c_1, c_2 \leftarrow$ Processing cost and waiting cost for event triggered data frames.
$C_{ET}(\mu), C_{RT}(\mu) \leftarrow$ Service costs for ETVF and RTVF.
foreach $i = 1$ *to* n **do**
  Estimate: $\langle\lambda_i\rangle, \langle\mu_i\rangle$
end
Compute:
$P_x(t) = \frac{e^{-\lambda t}(\lambda t)^x}{x!}$;
$f(t) = \mu e^{-\mu t}$;
$C_{ET}(\mu) = c_1\mu + c_2\left(\frac{\lambda}{\mu-\lambda}\right)$;
$C_{RT}(\mu) = c_1\mu + c_2\left[\frac{k+1}{2k}\frac{\lambda^2}{\mu(\mu-\lambda)} + \frac{\lambda}{\mu}\right]$;
exit

4. Autocorrelation function

In this paper, the autocorrelation (AC) function is employed over the considered COVID-19 dataset pertaining to the number of confirmed cases, patients recovered, and deaths reported over a specific interval of time. For our analysis, we have considered the data for COVID-19 cases reported between 1 March 2020 and 28 August 2020. Therefore, in this scenario, autocorrelation analysis can be useful to characterize the correlation of sample data in convergence with a delayed replica of itself expressed as a function of delay (or lag) (Bebortta & Senapati, 2022). If we consider a time series X_i such that $i = 1, 2, \ldots, n$ to be a stochastic process pertaining to the number of confirmed cases, recovered cases, and deaths reported from COVID-19. Then, for some time lag t, the dependency between the observed time series X_i and the delayed time series X_{i-t} can be expressed as (Bebortta & Senapati, 2022),

$$\rho_t = \frac{Cov\left(X_i, X_{i-t}\right)}{\sqrt{Var\left(X_i\right) * Var\left(X_{i-t}\right)}} \tag{14}$$

In Eq. (14), the autocorrelation for an observed sample data is obtained, where $t = 1, 2, \ldots (n-1)$. The autocorrelation function exhibits peculiar characteristics of decay in the sample's correlation after a certain time lag and hence can be used for modeling short memory processes. It indicates that X_i becomes independent for large values of t. Hence, such models can play a significant role in the temporal characterization of COVID-19 cases and predict future incidences of COVID-19 by considering data samples from the past few days.

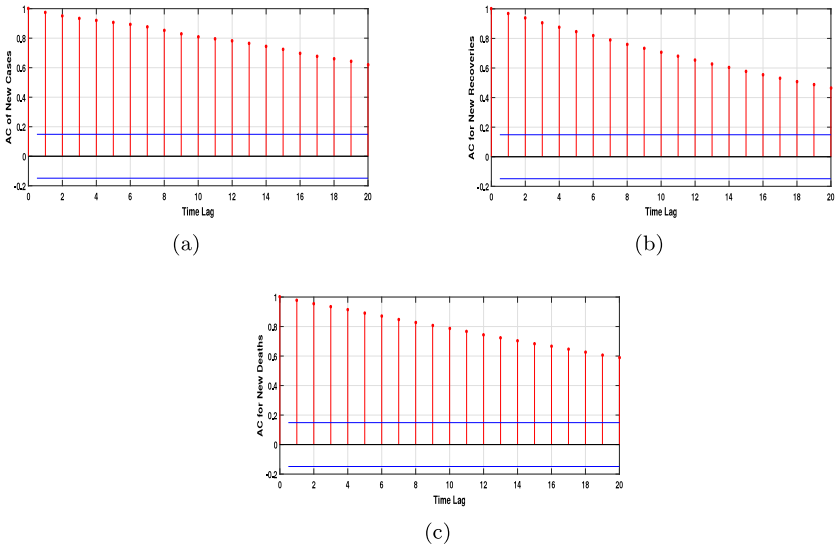

Fig. 6. (a) Autocorrelation analysis for number of confirmed COVID-19 cases. (b) Autocorrelation analysis for number of new recovered cases. (c) Autocorrelation analysis for number of new deaths reported.

5. Results and discussions

In this section, the results for the case study of India are presented. The COVID-19 data for India is collected from Kaggle between the duration of 1 March 2020 and 28 August 2020 (https://www.kaggle.com/sudalairajkumar/covid19-in-india). Autocorrelation analysis has been performed over the considered dataset for the number of confirmed cases, recovery rate, and COVID-19 deaths reported in India. The results corresponding to the spread of COVID-19 cases pertaining to confirmed, recovered, and death cases in a state-wise manner are presented which indicates the distribution of cases in India from a spatial perspective. These results can be observed through choropleth density maps as provided in this study with the respective number of cases reported in each region. Further, numerical results corresponding to proposed ETVF and RTVF models have been provided, and the respective service costs for each model are presented in a stratified manner.

5.1. Autocorrelation analysis

Autocorrelation analysis has been performed upon the time series data corresponding to the number of newly confirmed COVID-19 cases, the number of patients recovered, and the number of COVID-19 deaths reported in India. In Fig. 6(a), autocorrelation analysis results corresponding to the number of new confirmed COVID-19 cases reported in India between 1 March 2020 and 28 August 2020 are presented. Fig. 6(b), provides autocorrelation analysis for the number of patients recovered between the specified time period. Finally, autocorrelation analysis for the number of deaths reported from COVID-19 is represented in Fig. 6(c).

5.2. Spatial analysis of COVID-19 cases

We have performed a spatial analysis of COVID-19 cases in India, corresponding to each state. This assists in obtaining an insight into the spatial distribution of COVID-19 cases in India and their transmission patterns. Choropleth analysis has been performed over the cumulative confirmed cases, recovered cases, and deaths reported in respective states as of 28 August 2020. We have employed Python 3.8.2 to generate the respective maps using `geopandas` library. In Fig. 7(a), the choropleth map for confirmed COVID-19 cases corresponding to respective states is provided. The cumulative number of recovered cases pertaining to each state is represented in Fig. 7(b). The choropleth maps for COVID-19 deaths reported in each state are presented in Fig. 7(c).

5.3. Experimental setup

This section deals with the experimental setup for the considered social distancing framework along with a face recognition and contactless temperature monitoring module. The setup comprises of a mobile workstation with Intel i7-9750H processor, a Raspberry pi 5MP camera module, and an MLX 90614 contactless temperature sensor module. We have adopted the HoG framework over OpenCV platform to act as an indicator for real-time human body detection. Further, the HaarCascade and LBPH algorithms have been conjectured to facilitate real-time identification of the participants involved in the experiment and their respective temperatures. The threshold for normal human body temperature has been considered to be 98° F, exceeding which leads to the generation of an alert signal to the users' interface.

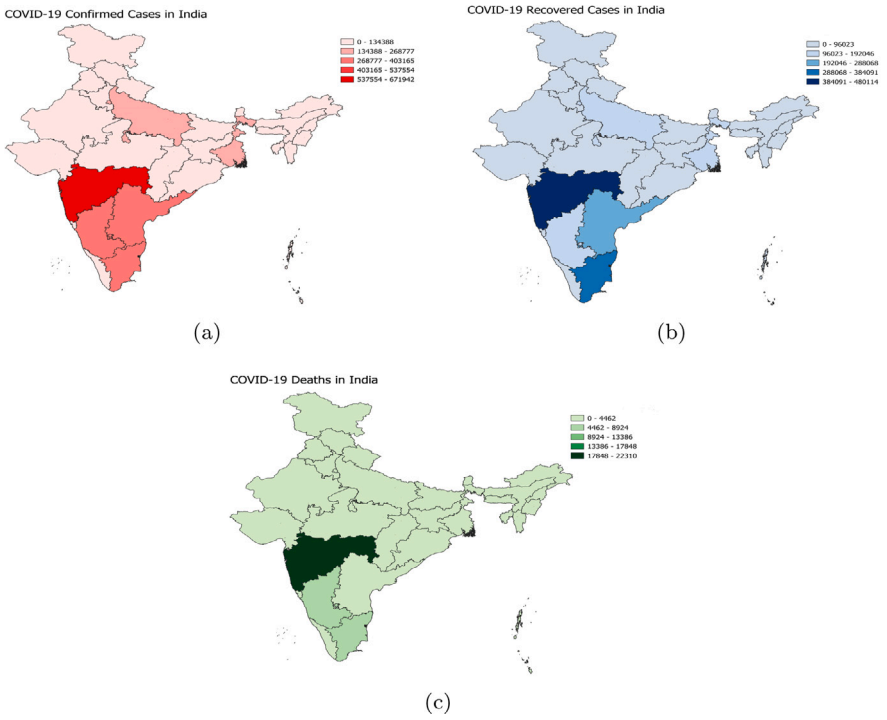

Fig. 7. (a) Statewise choropleth analysis of confirmed cases in India. (b) Choropleth analysis for recovery rate corresponding to individual states. (c) Choropleth analysis for cumulative deaths reported for each state.

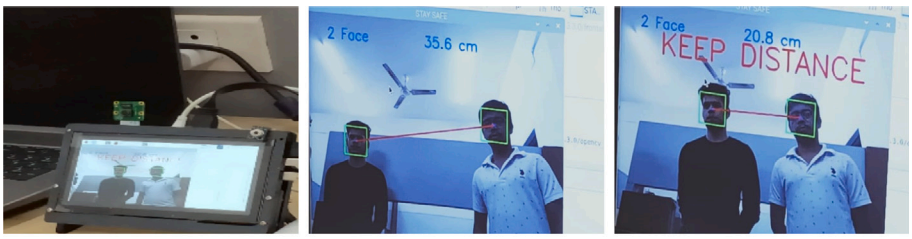

Fig. 8. (a) depicts the experimental setup for capturing distance between observed participants. (b) represents the two participants at a safe social distance range from one another. (c) depicts the violation of social distancing and displays the alert screen for the implemented module.

From Fig. 8(a), the experimental setup for the deployed module can be observed. In Fig. 8(b), the distance between two participants is captured which comes under the required safe distance range. Fig. 8(c), depicts the instance for violation of social distancing norms by the two participants for the considered real-time scenario. Fig. 9 provides the overview for face recognition and thermal screening module. This module comprises of a user specified database representing specific identified user and displays their names as entered in the database along with their temperature in real-time. The unidentified users, or the participants not included in the database are identified as unknown and only their temperature and captured face is displayed in the user's interface in real-time. In Fig. 9(a), the result depicting the user's interface for a recognized participant along with the body temperature and name as identified from the user's database is provided. Further, Fig. 9(b) provides the interface captured for an unidentified participant along with temperature of that participant. The proposed module leverages fast identifications of the identified participants and hence may have several real-world applicability in compliance to contact tracing and distancing monitoring schemes.

5.4. Numerical results

In this section, we provide the numerical results obtained for proposed ETVF model and compare those results with RTVF model. The trade-offs between both the models have been provided for different parameters. We have compared numerical results obtained for ETVF model to evaluate its performance for different service rates. Fig. 10(a) provides the service cost estimates for ETVF model obtained when $\mu = [10 : 30]$, $c1 = 5$, $c2 = 6$, and the reduction factor $k = 15$ for different values of λ i.e., for $\lambda = 8, 8.2, 8.4, 8.6$.

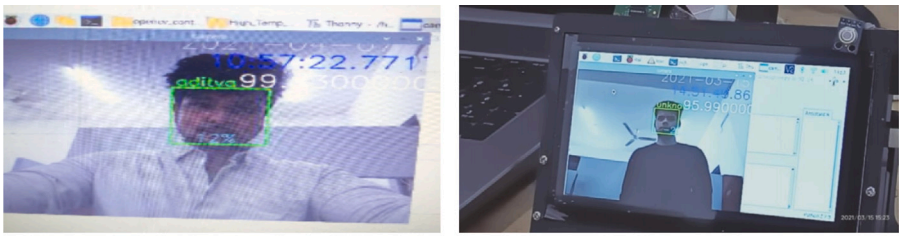

Fig. 9. (a) shows the face captured for a known subject along with its temperature. (b) represents the face and temperature of an unidentified subject.

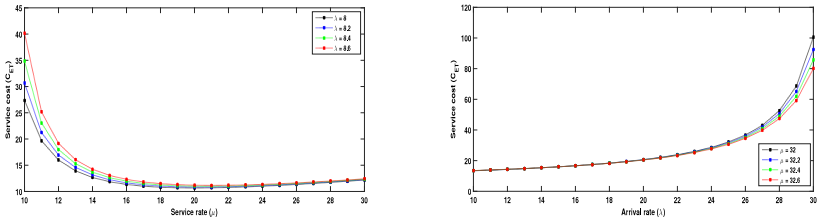

Fig. 10. Service cost for ETVF with different arrival rates and service rates. (a) The service cost for different values of λ i.e., $\lambda = 8, 8.2, 8.4, 8.6$. (b) The service cost for different values of μ i.e., $\mu = 32, 32.2, 32.4, 32.6$.

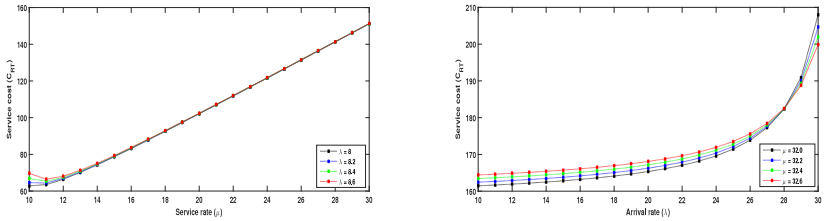

Fig. 11. Service cost for RTVF with different arrival rates and service rates. (a) The service cost for different values of λ i.e., $\lambda = 8, 8.2, 8.4, 8.6$. (b) The service cost for different values of μ i.e., $\mu = 32, 32.2, 32.4, 32.6$.

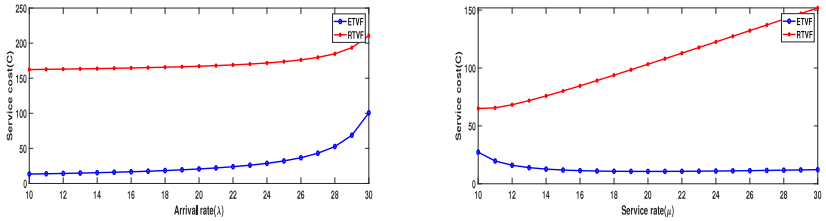

Fig. 12. (a) The service cost of ETVF and RTVF models corresponding to its arrival rates (i.e., $\lambda = [10 : 30]$), $k = 15$, $\mu = 32$, $c1 = 5$, and $c2 = 6$) and (b) the service cost of both models corresponding to its service rates (i.e., $\mu = [10 : 30]$), $k = 15$, $\lambda = 8$, $c1 = 5$, and $c2 = 6$.

Fig. 10(b) provides the service cost estimates by considering stable parameters $c1 = 5$, $c2 = 6$, and $k = 15$ obtained when $\lambda = [10 : 30]$ for different values of μ i.e., $\mu = 32, 32.2, 32.4, 32.6$. Fig. 11 provides the service cost for RTVF model with parameters, $k = 15$, $c1 = 5$, $c2 = 6$, where Fig. 11(a) provides the service cost for $\mu = [10 : 30]$ with different arrival rates i.e., $\lambda = 8, 8.2, 8.4, 8.6$ and Fig. 11(b) provides the service cost when $\lambda = [10 : 30]$ for different values of μ viz., $\mu = 32, 32.2, 32.4, 32.6$.

Fig. 12 provides the performance trade-offs between proposed ETVF model and RTVF model. The stable parameters considered in this case are as follows: $k = 15$, $c1 = 5$, and $c2 = 6$. Fig. 12a provides the service costs of ETVF and RTVF model for $\lambda = [10 : 30]$ and service rate $\mu = 32$. Fig. 12(b) provides the service costs for ETVF and RTVF model for dynamic parameters $\mu = [10 : 30]$ and arrival rate $\lambda = 8$.

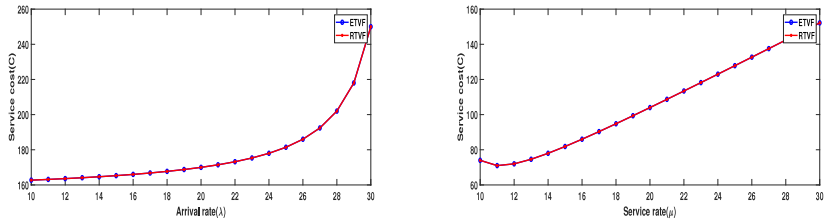

Fig. 13. For $k = 1$, (a) the service cost of ETVF and RTVF models corresponding to its arrival rates (i.e., $\lambda = [10 : 30]$), $\mu = 32$, $c1 = 5$, and $c2 = 6$) and (b) the service cost of both models corresponding to its service rates (i.e., $\mu = [10 : 30]$), $\lambda = 8$, $c1 = 5$, and $c2 = 6$.

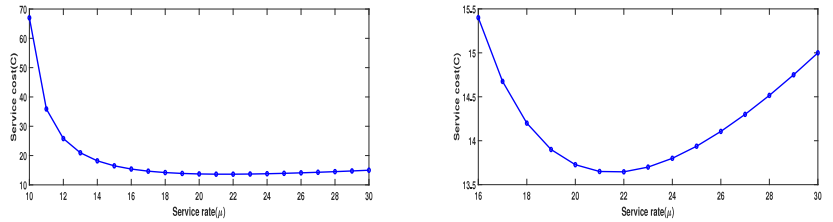

Fig. 14. (a) The service cost of ETVF a corresponding to its service rates (i.e., $\mu = [10 : 30]$), $k = 15$, $\lambda = 9$, $c1 = 6$, and $c2 = 7$) and (b) shows that the Fig.(a) attains its optimal value at $\mu = 22$.

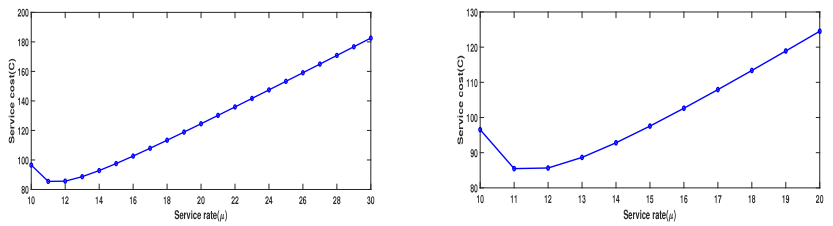

Fig. 15. (a) The service cost of RTVF a corresponding to its service rates (i.e., $\mu = [10 : 30]$), $k = 15$, $\lambda = 9$, $c1 = 6$, and $c2 = 7$) and (b) shows that the Fig.a attains its optimal value at $\mu = 11$.

Fig. 13 provides the service cost estimation corresponding to ETVF and the RTVF approach for transmission of data frame when the reduction factor k takes a unit value i.e., for $k = 1$. In Fig. 13(a) the parameters considered are $\lambda = [10 : 30]$, $\mu = 32$, $c1 = 5$ and $c2 = 6$. Further Fig. 13(b) considers the parameters $\mu = [10 : 30]$, $\lambda = 8$, $c1 = 5$, and $c2 = 6$ for obtaining the service costs. It would be striking to observe that the previous results considered a reduction factor of $k = 15$, thus resulting in considerable performance trade-offs between two models. However when the risk factor takes a unit value i.e., $k = 1$, the two models (i.e., ETVF and RTVF models) converge hence indicating parallel performance for the reduced value of reduction factor corresponding to the patients being infected with COVID-19.

Fig. 14(a) provides the service costs for the proposed ETVF model for different parameters viz., $\mu = [10 : 30]$, $k = 15$, $\lambda = 9$, $c1 = 6$, and $c2 = 7$. Fig. 14(b) represents a windowed view for the optimal value obtained from Fig. 11(a). It is observed that the model provides an optimal value when service rate $\mu = 22$ resulting in a service cost of $C_{ET} = 13.64$. In Fig. 15(a), the service cost for RTVF model has been provided. The parameters considered for obtaining the service cost corresponding to RTVF model are as follows: $\mu = [10 : 30]$, $k = 15$, $\lambda = 9$, $c1 = 6$, and $c2 = 7$. Fig. 15(b) provides the windowed view for optimal value of RTVF model which is obtained at $\mu = 11$ and the corresponding service cost is $C_{RT} = 85.47$. The service cost for the RTVF model continues to grow after this point. Hence it is observed that the proposed ETVF model obtains much optimal service cost i.e., $C_{ET} = 13.64$ for service rate $\mu = 22$. Table 1 provides a detailed summary of the service costs for ETVF model obtained for different values of μ. In Table 2 the respective values for service cost of the RTVF model is provided corresponding to different values of service rate μ. The optimal cost model pertaining to the proposed framework provides the optimal operating service cost for processing the captured facial data over the local computing device. The objective of computing the optimal service cost is to prompt the application user working on the facial detection framework to judiciously utilize the computing resources for processing massive digital imageries captured and to minimize the overall processing cost.

Table 1
Service cost for ETVF model.

Service rate	*Service cost*	*Service rate*	*Service cost*	*Service rate*	*Service cost*	*Service rate*	*Service cost*
11	35.90	16	15.40	21	13.65	26	14.10
12	25.80	17	14.67	**22**	**13.64**	27	14.30
13	20.95	18	14.20	23	13.70	28	14.51
14	18.20	19	13.90	24	13.80	29	14.75
15	16.50	20	13.72	25	13.93	30	15

Table 2
Service cost for RTVF.

Service rate	*Service cost*	*Service rate*	*Service cost*	*Service rate*	*Service cost*	*Service rate*	*Service cost*
11	**85.47**	16	102.63	21	130.20	26	159.10
12	85.65	17	107.92	22	135.92	27	164.95
13	88.66	18	113.36	23	141.67	28	170.81
14	92.82	19	118.90	24	147.46	29	176.69
15	97.56	20	124.52	25	153.27	30	182.58

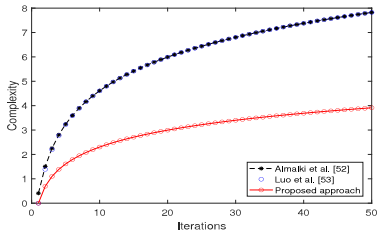

Fig. 16. Complexity analysis of proposed EVTF algorithm with some state-of-the-art approaches.

5.5. Complexity analysis

In order to assess the performance of the proposed EVTF algorithm, we compare it with two state-of-the-art models used for human movement tracking during COVID-19 (Almalki, Alotaibi, & Angelides, 2021; Luo, Gee, Piccoli, Work, & Samaranayake, 2022). Fig. 16, illustrates the complexity of the proposed EVTF algorithm for different iterations. It is observed that the proposed model outperforms the computational complexity of state-of-the-art algorithms, i.e., the proposed model is in linear order $O(n)$, whereas the model in Almalki et al. (2021) Luo et al. (2022), falls under the category of quadratic order $O(n^2)$. Therefore, The proposed method performs well and incurs fast computation for monitoring and recognition systems in a broader sense.

6. Related work

The high transmission rate and risk factors affecting a large population across countries with COVID-19 has alarmed the government organizations to take stringent actions to curb its spread. However, due to lack of sufficient mechanism to mitigate the transmission of the pandemic, more recently emerging intelligent technologies have become popular towards this end. In Cabani, Hammoudi, Benhabiles, and Melkemi (2021), an image editing strategy for three different types of face mask detection was proposed. Their model was categorized into three classes namely, correctly masked, incorrectly masked, and global masked face recognition. The primary objective was to detect whether the population under consideration appropriately used face masking. In Das, Ansari, and Basak (2020), the authors employed OpenCV, TensorFlow, and Keras for facial detection and face masking for stationary as well as motion condition. Their framework leveraged sequential convolutional neural network (SCNN) model for appropriate detection of masking and facial recognition without the chances of overfitting. The work in Ahmed, Ahmad, Rodrigues, Jeon, and Din (2021), explored a transfer learning framework for tracking social distancing subject to a violation threshold. The physical distance between the participants and pixel was approximated to decide the threshold for social distancing. Further, they also proposed a tracking algorithm for detecting individuals in video sequences, to track for violations.

As a consequence of lack of availability of standardized dataset and their collection, the applications of deep transfer learning was considered to be profound (Sufian, Ghosh, Sadiq, & Smarandache, 2020). Here, IoT-based devices and edge computing services also play an important role in data acquisition, processing and storage. Hence, the transfer learning approach presented in Sufian et al. (2020), for tracking social distancing policies was considered to be pivotal for IoT devices with limited processing capabilities. The study in Saponara, Elhanashi, and Gagliardi (2021), developed social distancing strategies based on thermal camera images for controlling transmission of COVID-19. Their system encompassed mobility monitoring module, categorization of social distancing policies, and body temperature monitoring through thermal camera module. The Ground truth labeler app was employed to label people in capture images. Hence, their approach has applications for distributed surveillance systems.

7. Conclusion and future directions

The coronavirus pandemic has been wreaking havoc in the entire world. The disease spreads when a person comes in direct contact with the infected individual or the objects that the infected person has touched. The only possible remedy for the deadly situation is avoiding the crowd and self-imposed or the advised quarantine that keeps the person away from the healthy mass and curbs the infection rate. The proposed real-time smart screening facility based on event-triggered image capture and drone computing-based digital forensic architecture using the human detection and facial recognition algorithm have been presented, which can serve the role as a monitoring platform for tracking the infection and the social distancing which not only reduces the human exposure and checks the spread of the disease but also reduces the service cost in comparison to the real-time video framing. Further, we have compared the performance of the proposed ETVF model with the conventional RTVF model. It is observed that the proposed ETVF model outperforms the RTVF model and obtains an optimal value at $\mu = 22$ with a service cost of $C_{ET} = 13.64$ for processing the captured video frames. We presented the results for autocorrelation function pertaining to different cases of COVID-19 ($viz.$, number of confirmed COVID-19 cases, recovered patients, and deaths) are provided for the case study of India. We have also performed choropleth analysis for the above scenarios, which provides a visualization of the magnitude of COVID-19 cases in a state-wise manner. Finally, the computational complexity of the proposed approach was compared with some state-of-the-art human movement traacking algorithms where the proposed approach was observed to outperform the computational complexity by considering a linear complexity of the order $O(n)$ for processing the video frames.

Although the integration of some cutting-edge technologies like the Internet of Things (IoT) enabled smart city monitoring, drone-based surveillance drives, biometrics authentication, etc., have constantly favored the e-governance framework. It has also improved the government's services towards the citizens proactively. However, there are still several scopes for improving the optimal usage of these resources and their efficacy in administering numerous authoritative tasks. Further, by combining these smart frameworks along with some analytical models numerous public safety management prototypes can be developed.

CRediT authorship contribution statement

Sujit Bebortta: Conceptualization, Software, Validation, Investigation, Data curation, Writing – original draft, Writing – review & editing. **Aditya Ranjan Dalabehera:** Methodology, Software, Validation, Visualization, Writing – review & editing. **Bibudhendu Pati:** Conceptualization, Resources, Writing – review & editing. **Chhabi Rani Panigrahi:** Conceptualization, Resources, Writing – review & editing. **Gyana Ranjan Nanda:** Writing – review & editing, Visualization. **Biswajit Sahu:** Writing – review & editing, Visualization. **Dilip Senapati:** Conceptualization, Methodology, Software, Validation, Formal analysis, Investigation, Data curation, Writing – original draft, Supervision, Project administration.

Declaration of competing interest

The authors declare that they have no known competing financial interests or personal relationships that could have appeared to influence the work reported in this paper.

Data availability

No data was used for the research described in the article.

Acknowledgments

The authors would like to thank the anonymous reviewers for their thoughtful comments, which assisted in improving the overall quality of this article. The authors also would like to express their gratitude to OURIIP, Odisha, India, for providing the necessary research environment and extending their support to initiate the project under Grant No. 28Seed/2019/Comp. Sc. And Engg.-5.

References

Ahmed, I., Ahmad, M., Rodrigues, J. J., Jeon, G., & Din, S. (2021). A deep learning-based social distance monitoring framework for COVID-19. *Sustainable Cities and Society*, *65*, Article 102571.

Ahonen, T., Hadid, A., & Pietikainen, M. (2006). Face description with local binary patterns: Application to face recognition. *IEEE Transactions on Pattern Analysis and Machine Intelligence*, *28*(12), 2037–2041.

Almalki, F. A., Alotaibi, A. A., & Angelides, M. C. (2021). Coupling multifunction drones with AI in the fight against the coronavirus pandemic. *Computing*, 1–27.

Bebortta, S., & Das, S. K. (2020). Assessing the impact of network performance on popular E-learning applications. In *2020 Sixth international conference on e-learning (Econf)* (pp. 61–65). IEEE.

Bebortta, S., Panda, M., & Panda, S. (2020). Classification of pathological disorders in children using random forest algorithm. In *2020 International conference on emerging trends in information technology and engineering (Ic-ETITE)* (pp. 1–6). IEEE.

Bebortta, S., Rajput, N. K., Pati, B., & Senapati, D. (2020). A real-time smart waste management based on cognitive IoT framework. In *Advances in electrical and computer technologies* (pp. 407–414). Springer.

Bebortta, S., & Senapati, D. (2021a). A secure blockchain-based solution for harnessing the future of smart healthcare. In *IoT-Based data analytics for the healthcare industry* (pp. 167–191). Elsevier.

Bebortta, S., & Senapati, D. (2021b). Empirical characterization of network traffic for reliable communication in IoT devices. In *Security in cyber-physical systems* (pp. 67–90). Springer.

Bebortta, S., & Senapati, D. (2022). Characterizing the epidemiological dynamics of COVID-19 using a non-parametric framework. *Current science*, *122*(7), 790.
Bebortta, S., Senapati, D., Panigrahi, C. R., & Pati, B. (2021a). An adaptive modeling and performance evaluation framework for edge-enabled green IoT systems. *IEEE Transactions on Green Communications and Networking*, *6*(2), 836–844.
Bebortta, S., Senapati, D., Panigrahi, C. R., & Pati, B. (2021b). An adaptive performance modeling framework for QoS-aware offloading in MEC-based IIoT systems. *IEEE Internet of Things Journal*.
Bebortta, S., Senapati, D., Rajput, N. K., Singh, A. K., Rathi, V. K., Pandey, H. M., et al. (2020). Evidence of power-law behavior in cognitive IoT applications. *Neural Computing and Applications*, 1–13.
Bebortta, S., & Singh, S. K. (2021). An adaptive machine learning-based threat detection framework for industrial communication networks. In *2021 10th IEEE International conference on communication systems and network technologies (CSNT)* (pp. 527–532). IEEE.
Bebortta, S., & Singh, S. K. (2022a). An intelligent framework towards managing big data in internet of healthcare things. In *International conference on computational intelligence in pattern recognition* (pp. 520–530). Springer.
Bebortta, S., & Singh, S. K. (2022b). An opportunistic ensemble learning framework for network traffic classification in IoT environments. In *Proceedings of the seventh international conference on mathematics and computing* (pp. 473–484). Springer.
Bebortta, S., Singh, A. K., Mohanty, S., & Senapati, D. (2020). Characterization of range for smart home sensors using tsallis' entropy framework. In *Advanced computing and intelligent engineering* (pp. 265–276). Springer.
Bebortta, S., Singh, A. K., Pati, B., & Senapati, D. (2021). A robust energy optimization and data reduction scheme for IoT based indoor environments using local processing framework. *Journal of Network and Systems Management*, *29*(1), 1–28.
Bebortta, S., Singh, A. K., & Senapati, D. (2022). Performance analysis of multi-access edge computing networks for heterogeneous IoT systems. *Materials Today: Proceedings*, *58*, 267–272.
Boland, G. F., Kozloski, J. R., Ma, Y., Manweiler, J. G., Siemonsen, K. E., Topkara, U., et al. (2020). System and method to operate a drone. US Patent 10, 545, 512.
Bold, S., Sosorbaram, B., & Lee, S. R. (2016). Implementation of autonomous unmanned aerial vehicle with moving-object detection and face recognition. In *Information science and applications (ICISA) 2016* (pp. 361–370). Springer.
Buizza, R. (2020). Probabilistic prediction of COVID-19 infections for China and Italy, using an ensemble of stochastically-perturbed logistic curves. arXiv preprint arXiv:2003.06418.
Cabani, A., Hammoudi, K., Benhabiles, H., & Melkemi, M. (2021). MaskedFace-Net–A dataset of correctly/incorrectly masked face images in the context of COVID-19. *Smart Health*, *19*, Article 100144.
Cuimei, L., Zhiliang, Q., Nan, J., & Jianhua, W. (2017). Human face detection algorithm via haar cascade classifier combined with three additional classifiers. In *2017 13th IEEE international conference on electronic measurement & instruments (ICEMI)* (pp. 483–487). IEEE.
Das, A., Ansari, M. W., & Basak, R. (2020). Covid-19 face mask detection using TensorFlow, Keras and OpenCV. In *2020 IEEE 17th india council international conference (INDICON)* (pp. 1–5). IEEE.
Das, S. K., & Bebortta, S. (2022). A study on geospatially assessing the impact of COVID-19 in Maharashtra, India. *The Egyptian Journal of Remote Sensing and Space Science*, *25*(1), 221–232.
Davis, M., & Sahin, F. (2016). HOG feature human detection system. In *2016 IEEE international conference on systems, man, and cybernetics (SMC)* (pp. 002878–002883). IEEE.
Ditlevsen, S., & Samson, A. (2013). Introduction to stochastic models in biology. In *Stochastic biomathematical models* (pp. 3–35). Springer.
Domingues, P., & Rosário, A. F. (2019). Deep learning-based facial detection and recognition in still images for digital forensics. In *Proceedings of the 14th international conference on availability, reliability and security* (pp. 1–10).
Fan, X., Zhang, F., Wang, H., & Lu, X. (2012). The system of face detection based on OpenCV. In *2012 24th Chinese control and decision conference (CCDC)* (pp. 648–651). IEEE.
Garfinkel, S. L. (2010). Digital forensics research: The next 10 years. *Digital Investigation*, *7*, S64–S73.
Goel, N. S., & Richter-Dyn, N. (2016). *Stochastic models in biology*. Elsevier.
Guan, W.-j., Ni, Z.-y., Hu, Y., Liang, W.-h., Ou, C.-q., He, J.-x., et al. (2020). Clinical characteristics of coronavirus disease 2019 in China. *New England Journal of Medicine*, *382*(18), 1708–1720.
Hsu, H.-J., & Chen, K.-T. (2015). Face recognition on drones: Issues and limitations. In *Proceedings of the first workshop on micro aerial vehicle networks, systems, and applications for civilian use* (pp. 39–44).
Hu, Y., Delbruck, T., & Liu, S.-C. (2020). Exploiting event cameras by using a network grafting algorithm. arXiv preprint arXiv:2003.10959.
Huang, C., Wang, Y., Li, X., Ren, L., Zhao, J., Hu, Y., et al. (2020). Clinical features of patients infected with 2019 novel coronavirus in Wuhan, China. *The Lancet*, *395*(10223), 497–506.
Iqbal, F., Alam, S., Kazim, A., MacDermott, A., et al. (2019). Drone forensics: A case study on DJI phantom 4. In *2019 IEEE/ACS 16th International conference on computer systems and applications (AICCSA)* (pp. 1–6). IEEE.
Lau, L. J., & Xiong, Y. (2020). Don't panic, be cautious, and together we can stop the coronavirus epidemic!. *Asia-Pacific Biotech News*, *24*(Supp01), 90–107.
Li, Q., Guan, X., Wu, P., Wang, X., Zhou, L., Tong, Y., et al. (2020). Early transmission dynamics in Wuhan, China, of novel coronavirus–infected pneumonia. *New England Journal of Medicine*.
Luo, Q., Gee, M., Piccoli, B., Work, D., & Samaranayake, S. (2022). Managing public transit during a pandemic: The trade-off between safety and mobility. *Transportation Research Part C (Emerging Technologies)*, *138*, Article 103592.
Mathur, S., Subramanian, B., Jain, S., Choudhary, K., & Prabha, D. R. (2017). Human detector and counter using raspberry pi microcontroller. In *2017 Innovations in power and advanced computing technologies (I-PACT)* (pp. 1–7). IEEE.
Mirzaeinia, A., Hassanalian, M., Lee, K., & Mirzaeinia, M. (2019). Energy conservation of V-shaped swarming fixed-wing drones through position reconfiguration. *Aerospace Science and Technology*, *94*, Article 105398.
Monforte, M., Arriandiaga, A., Glover, A., & Bartolozzi, C. (2020). Exploiting event-driven cameras for spatio-temporal prediction of fast-changing trajectories. arXiv preprint arXiv:2001.01248.
Motlagh, N. H., Bagaa, M., & Taleb, T. (2017). UAV-based IoT platform: A crowd surveillance use case. *IEEE Communications Magazine*, *55*(2), 128–134.
Mukherjee, T., Nayak, G., & Senapati, D. (2021). Evaluation of symbol error probability using a new tight Gaussian Q approximation. *International Journal of Systems, Control and Communications*, *12*(1), 60–71.
Mukherjee, T., Pati, B., & Senapati, D. (2020). Performance evaluation of composite fading channels using q-Weibull distribution. In *Progress in advanced computing and intelligent engineering* (pp. 317–324). Springer.
Mukherjee, T., & Senapati, D. (2022). An adaptive q-lognormal model towards the computation of average channel capacity in slow fading channels. *Telecommunication Systems*, *79*(3), 341–355.
Mukherjee, T., Singh, A. K., & Senapati, D. (2019). Performance evaluation of wireless communication systems over Weibull/q-lognormal shadowed fading using tsallis' entropy framework. *Wireless Personal Communications*, *106*(2), 789–803.
Nayak, G., Singh, A. K., & Senapati, D. (2020). Computational modeling of non-Gaussian option price using non-extensive tsallis' entropy framework. *Computational Economics*, 1–19.
Nguyen, D. T., Li, W., & Ogunbona, P. O. (2016). Human detection from images and videos: A survey. *Pattern Recognition*, *51*, 148–175.

Nguyen, H. D., Na, I. S., Kim, S. H., Lee, G. S., Yang, H. J., & Choi, J. H. (2019). Multiple human tracking in drone image. *Multimedia Tools and Applications*, *78*(4), 4563–4577.

Organization, W. H., et al. (2020). *Infection prevention and control during health care when novel coronavirus (nCoV) infection is suspected: interim guidance, January 2020*: *Tech. rep*, World Health Organization.

Peng, P. W., Ho, P.-L., & Hota, S. S. (2020). Outbreak of a new coronavirus: what anaesthetists should know. *BJA: British Journal of Anaesthesia*, *124*(5), 497.

Quick, D., & Choo, K.-K. R. (2014). Impacts of increasing volume of digital forensic data: A survey and future research challenges. *Digital Investigation*, *11*(4), 273–294.

Sahoo, H., Senapati, D., Thakur, I. S., & Naik, U. C. (2020). Integrated bacteria-algal bioreactor for removal of toxic metals in acid mine drainage from iron ore mines. *Bioresource Technology Reports*, *11*, Article 100422.

Sahu, K. K., Mishra, A. K., & Lal, A. (2020). Comprehensive update on current outbreak of novel coronavirus infection (2019-nCoV). *Annals of Translational Medicine*.

Saika, S., Takahashi, S., Takeuchi, M., & Katto, J. (2016). Accuracy improvement in human detection using HOG features on train-mounted camera. In *2016 IEEE 5th global conference on consumer electronics* (pp. 1–2). IEEE.

Saponara, S., Elhanashi, A., & Gagliardi, A. (2021). Implementing a real-time, AI-based, people detection and social distancing measuring system for Covid-19. *Journal of Real-Time Image Processing*, *18*(6), 1937–1947.

Sarkodie, S. A., & Owusu, P. A. (2020). Investigating the cases of novel coronavirus disease (COVID-19) in China using dynamic statistical techniques. Available At SSRN 3559456.

Seemanthini, K., & Manjunath, S. (2018). Human detection and tracking using HOG for action recognition. *Procedia Computer Science*, *132*, 1317–1326.

Senapati, D., et al. (2016). Generation of cubic power-law for high frequency intra-day returns: Maximum Tsallis entropy framework. *Digital Signal Processing*, *48*, 276–284.

Singh, A. K., Senapati, D., Bebortta, S., & Rajput, N. K. (2019). A non-stationary analysis of erlang loss model. In *Progress in advanced computing and intelligent engineering* (pp. 286–294). Springer.

Singh, A. K., Senapati, D., Mukherjee, T., & Rajput, N. K. (2019). Adaptive applications of maximum entropy principle. In *Progress in advanced computing and intelligent engineering* (pp. 373–379). Springer.

Singh, V., Shokeen, V., & Singh, B. (2013). Face detection by haar cascade classifier with simple and complex backgrounds images using opencv implementation. *International Journal of Advanced Technology in Engineering and Science*, *1*(12), 33–38.

Singhal, T. (2020). A review of coronavirus disease-2019 (COVID-19). *The Indian Journal of Pediatrics*, *87*(4), 281–286.

Sufian, A., Ghosh, A., Sadiq, A. S., & Smarandache, F. (2020). A survey on deep transfer learning to edge computing for mitigating the COVID-19 pandemic. *Journal of Systems Architecture*, *108*, Article 101830.

Team, E. (2020). The epidemiological characteristics of an outbreak of 2019 novel coronavirus diseases (COVID-19)—China, 2020. *China CDC Weekly*, *2*(8), 113.

Trivedi, K. S. (2008). *Probability & statistics with reliability, queuing and computer science applications*. John Wiley & Sons.

Unlu, E., Zenou, E., Riviere, N., & Dupouy, P.-E. (2019). An autonomous drone surveillance and tracking architecture. *Electronic Imaging*, *2019*(15), 35–351.

Visakha, K., & Prakash, S. S. (2018). Detection and tracking of human beings in a video using haar classifier. In *2018 International conference on inventive research in computing applications (ICIRCA)* (pp. 1–4). IEEE.

Wang, C., Horby, P. W., Hayden, F. G., & Gao, G. F. (2020). A novel coronavirus outbreak of global health concern. *The Lancet*, *395*(10223), 470–473.

Zhao, X., & Wei, C. (2017). A real-time face recognition system based on the improved LBPH algorithm. In *2017 IEEE 2nd international conference on signal and image processing (ICSIP)* (pp. 72–76). IEEE.